

# Wind Energy Conversion System using Predictive Control with Lyapunov Based Observer

<sup>1</sup> A.Durgadevi, <sup>2</sup> S.P.Richard, <sup>3</sup> K. Dhayalini

Assistant professor, Department of Electrical and Electronics Engineering, K. Ramakrishnan College of Engineering Tiruchirappalli, Tamil Nadu – 621 112, India.

durganathan8588@gmail.com, richard@krce.ac.in, dhaya2k@gmail.com

**Abstract**—Storm Power translation system is a reliable renewable power translation scheme. The generated power of wind energy translation system tends to fluctuate due to the wind mill production power is generally relative to the cube of wind velocity that is not always constant. An advanced control strategy must be used to provide the wind power output as maximum and more reliable. A novel control strategy, nonlinear generalized predictive control law in support of rotating side converter of two fold virtual Induction Alternator established storm turbine is designed. The control plan based on two loops: The inner Torque-Current control loop based on NGPC provides the rotor reference voltage toward the rotating side converter as well as the outer NGPC based velocity control loop supplies the suggestion electromagnetic torque to inner loop. To give amazing ability to handle system conflict and enhance robustness of the controller, an aerodynamic torque observer is designed which is considered as an unknown perturbation and integrated with NGPC controller. Finally, simulations are done using MATLAB/Simulink. Simulation results show the projected control strategy that maximizes the necessity of the WECS power output during variations in wind speed.

**Keywords**—Nonlinear Generalized Predictive Control (NGPC), Aerodynamic Torque Observer, Two Fold virtual Induction Alternator (TFVIA), Storm Power Translation System (SPTS).

## NOMENCLATURE

$\rho$	Air density
$P_t$	Power extracted from wind
$v$	Wind velocity
$\lambda_{opt}$	Optimal tip-speed ratio
$\Omega_t$	Turbine
$\Omega_r$	Alternator speed
$\Omega_{r\_ref}$	Reference Alternator speed
$C_p\_max$	Maximal power coefficient
$G$	Gear ratio
$J$	Moment of Inertia
$f_r$	Collusive of friction
$P_{grid\_ref}$	Reference grid Active power (W)
$\psi_s, \psi_r$	Stator and Rotor fluxes
$V_{ds}, V_{qs}$	2 $\phi$ stator voltages
$V_{qr}, V_{dr}$	2 $\phi$ rotor voltages
$I_{ds}, I_{qs}$	2 $\phi$ stator currents
$I_{dr}, I_{qr}$	2 $\phi$ rotor currents
$\psi_{ds}, \psi_{qs}$	2 $\phi$ stator fluxes
$\psi_{dr}, \psi_{qr}$	2 $\phi$ rotor fluxes
$P_s$	Stator Active power
$Q_s$	Stator Reactive Power
$P_r, Q_r$	Rotor Active and Reactive Power
$\omega_s, \omega_r$	Stator and Rotor Angular Velocities

$f(x), h(x),$  Capacities thought to be constantly

$g_u(x), g_T(x)$  Differentiable incessant Capacities of  $x$   
 $T_p$  Predictive time

## I. INTRODUCTION

As of late, the utilization of sustainable power assets has increased. Of the different elective fuel sources, wind energy being uninhibitedly accessible and non-contaminating, has been supported the world over as the most attainable and monetarily serious choice. Because of this, the infiltration of the wind energy in electrical power generating system is quickly increasing. The wound rotor induction mechanism commonly named as doubly fed induction generator which offers several advantages, is finding increasing application, especially in the variable speed wind energy transformation system. These points of interest counting speed control and four quadrant dynamic and responsive force abilities, are principally accomplished by means of controlling of a rotating side converter, that is normally evaluated at approximately 31%–36% for Alternator rating of a given rotor velocity deviation vary of  $\pm 24\%$  [1].

In doubly fed induction generator based airstream turbine, field oriented control principle for decoupled have power over the generator's active and reactive power using conventional PI controller is common which provides simplicity and pertinence [6]. However, PI type controller is not effectual when the system is subjected to the strong external disturbance. To overcome this problem an advanced control strategy, RST polynomial controller and LQG controllers are used to provide the maximum reliability. When the boundaries varieties of the DFIG increment, the time-reaction of the PI and RST regulator also increased, but the LQG controller does not have time response elapse [8]. Some of the adaptive controllers are also in research such as  $H_\infty$  control theory, sliding mode control and neural networks [9]. An advanced control strategy, Model Predictive Control (MPC) is an emerging technique which is robust next to boundaries varieties and fast dynamic response. In [12] a nonlinear predictive control law is proposed for multivariable scheme by Chen et. al depends on Taylor series expansion. The multi-input and multi-output scheme through equal relative degree is taken. In [13, 14], the direct torque control (DTC) integrated with MPC principle is useful to an induction motor (IM) to attain the rapid torque reaction. In [9], the weight torque is measured as a identified interruption with cascaded nonlinear generalized predictive control based on Taylor series expansion for an Rotating Transformer. In [16], to reduce power fluctuations by control the pitch angle of windmill blades the generalized predictive control erstwhile proposed. Multiple MPC control technique to maximize the output energy has been anticipated for wind turbine based DFIG in [17]. A prescient current control (PCC) technique for Two Fold virtual Induction Alternator erstwhile utilized in [18]. In every one of these strategies the external disturbance (streamlined force) is acknowledged one to high performance.

In order to achieve high performance and robustness against the unknown perturbation, an aerodynamic torque observer should integrate with nonlinear generalized predictive controller. Here, the performance index anticipated in [16] is estimated to build up the exhibitions of the DFIG-based breeze turbine under obscure aggravation and boundary varieties. The nonlinear generalized predictive controller is divided into control loops. The inner control loop called Torque-Current control loop is cascaded with the outer control loop called speed control loop. The aerodynamic torque is integrated with the cascaded NGPC controller.

## II. MODELING OF POWER TRANSLATION SYSTEMS

A WPTS is a arrangement that changes the motor power of the approaching air stream into electrical Power The energy transformation chain is coordinated into four subsystems [1]. *Aerodynamic subsystem* consists of turbine rotor which is collected by turbine hub and blades. Drive train commonly made out of low-velocity shaft combined with the turbine center, velocity multiplier and rapid shaft driving the Two Fold virtual Induction Alternator (TFVIA) Electromagnetic subsystem is established of the DFIG. Electric subsystem including the components for matrix association and nearby lattice via two pulse width modulated voltage source converter [4].

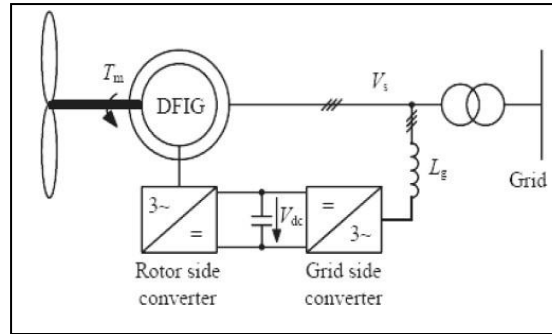


Fig. 1. Wind Energy Conversion System

**A. Storm Turbine Model**

The power extracted by a storm turbine whose blade length  $R$  is given as

$$P_t = \frac{1}{2} \rho A R^3 v^3 C_p(\lambda, \beta) \tag{1}$$

$$P_t = \frac{1}{2} \rho A R^3 v^3 C_p(\lambda, \beta)$$

The power coefficient ( $C_p$ ) explains the power extraction efficiency of a storm turbine is the role of both tip speed ratio ( $\lambda$ ) and pitch angle ( $\beta$ ). The tip speed ratio ( $\lambda$ ), is conventionally denoted here,

$$\lambda = \frac{\Omega_t R}{V} \tag{2}$$

The aerodynamic performance of a wind turbine is typically characterized by deviation of the non-dimensional coefficient of power versus tip speed ratio curve.

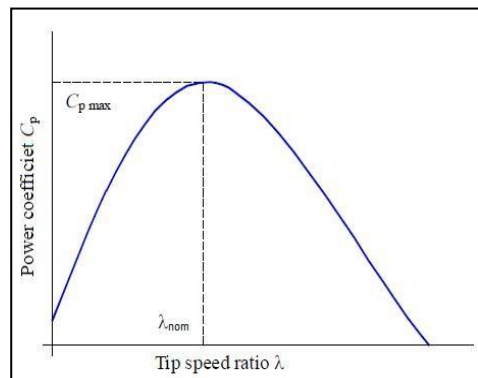


Fig. 2.  $C_p / \lambda$  curve

Theoretical renovation efficiency is determined by the Betz limit (0.59), but in general the conversion efficiency is determined by the value of  $C_p$ -max where  $C_p$  at the tip speed ratio  $\lambda_{nom}$ . At the end, the turbine ought to consistently function at  $\lambda_{nom}$ . For simplicity, eliminating the communication loss, the wind turbine torque and speed assigned to the generator side gearbox [2], are expressed as

$$T_G = T_t, \quad \Omega_G = \Omega_r \tag{3}$$

Substitute Equations (3) in Equations (2), the rotor speed is given by,

$$\Omega_{r-ref} = \lambda_{opt} v \tag{4}$$

R

In the grid side converter, to exploit the conversion efficiency grid power should maintain to the reference value. By substituting equation (3) in (1), the grid reference power is given by,



$$\frac{1}{2} \eta \rho \pi^2 v^3$$

Here  $\eta$  is the Storm turbine efficiency and  $\rho$  is the air density.

From equation (4) and (5), the rotating side reference velocity and the electrical grid reference power are obtained. This gridreference power ensures the maximum efficiency of the power transfer to the grid.

**B. Two Fold victual Induction Alternator modeling**

The TFVIA - based WECS are consisting of wound rotor mechanism which is perfunctorily attached to the wind turbine. The generator stator winding is openly joined to the grid combination transformer whereas the rotor winding is joined in the course of back to- back voltage supply converter. A dc-interface capacitor is associated between the Rotating Side Converter (RSC) and the matrix side converter (MSC) [3]. From the RSC, the wind generation is fully controlled while the outcome of the power is tracked with  $P_{grid-ref}$  through GSC by kept the dc- interface voltage constant.

The TFVIA can be described by d-q synchronous frame [8],if it is described by stator flux vector control principle, then the flux connected to the d-axis of the outline. Then we use stator flux linked with the q axis will be zero and total flux will be:

$$\psi_{ds} = 0, \text{ then } \psi_{qs} = \psi_s(6)$$

Now, the electromagnetic torque based on the q-axis rotor current.

$$T_{em} = p \frac{L_m V_s}{I} \omega_s L_s q_r(7)$$

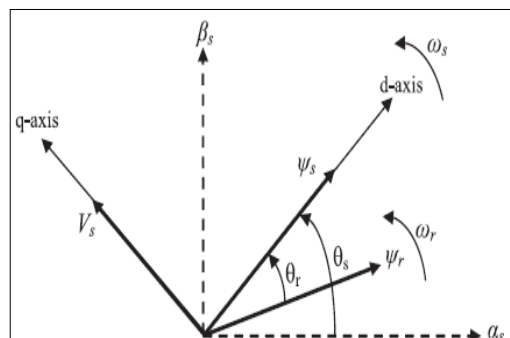


Fig. 3. V and flux vector diagram

As shown in fig. 3, the stator voltage vector is likewise in quadrature advance contrasted with the stator transition vector. Thus,the stator voltages are:

$$V_{ds} = 0, V_{qs} = V_s = \omega_s \psi_s(8)$$

Now, from the stator voltages, the rotor voltages are derived by,

$$V_{dr} = R_r I_{dr} + \sigma L_r \frac{d}{dt} I_{dr} - \sigma L_r s \omega_s I_{qr} \quad (9)$$

$$V_{qr} = R_r I_{qr} + \sigma L_r \frac{d}{dt} I_{qr} + \sigma s \omega_s I_{dr} - L_m V_s \quad (10)$$

Then the generator Stator active power and reactive power are articulated,

$$P_S = -L \frac{V_S}{I} \quad (11)$$
$$m L_S$$
$$q_r$$

$$Q_s = \frac{V^2}{\omega_s L_s} - L_m \frac{V}{L_s} I_r \quad (12)$$

The dispersion and generator slip ratio can be expressed as:

$$\sigma = 1 - \frac{L^2}{L_s L_r} \frac{\omega - \omega_s}{\omega_s}$$

### III. NONLINEAR GENERALIZED PREDICTIVE CONTROL LAW

Another nonlinear prescient control law for a class of multivariable nonlinear frameworks is introduced in this paper. It is demonstrated that the closed-loop elements under this nonlinear prescient regulator unequivocally based on plan boundaries.

Consider the nonlinear scheme:

$$\begin{aligned} \dot{x}(t) &= f(x(t)) + g_u(x(t))u(t) + \\ g_T(x(t))T_r(t) &= h_i(x(t)), \quad i = \\ 1, & \quad m(14) \end{aligned}$$

Where  $x \in R^n$ ,  $u \in R^m$  and  $y = [y_1; y_2; \dots; y_m]^T \in R^m$  are the state, control and yield vectors individually. In like manner, an ideal following issue can be expressed as follows: plan a regulator with the end goal that the shut circle framework is asymptotically steady so that state and the yield of the nonlinear framework (23), (24) ought to ideally tracks an endorsed reference,  $y_r(t)$ , regarding a given execution file [15].

The receding-horizon performance index given in [15] is adopted here, as follows:

$$J = \frac{1}{2} \int_0^T \{ [\hat{x}(t+\tau) - \hat{y}(t+\tau)]^T [ \hat{x}(t+\tau) - \hat{y}(t+\tau) ] \} \quad (15)$$

Like subsiding control methodologies, the genuine control input  $u(t)$ , is given by the underlying estimation of the ideal control input  $\hat{u}(t+\tau)$ ,  $0 \leq \tau \leq T$ , which minimizes the performance index (25) i.e., when  $\tau = 0$

$$u(t+\tau) = \hat{u}(t+\tau) \quad (16)$$

Finally, the essential state for the most advantageous control is given by

$$\frac{d\mu}{du} = 0 \quad (17)$$

### IV. CASCAD NGPC

As TFVIA is signalized by two scale modes i.e. electrical mode which is fast dynamics and electrical mode which is slow dynamics [2]. Two modes are adopted by cascaded structure. The interior circle is required to control the d-hub rotor current and the electromagnetic force, though the external circle is utilized for the velocity direction following.

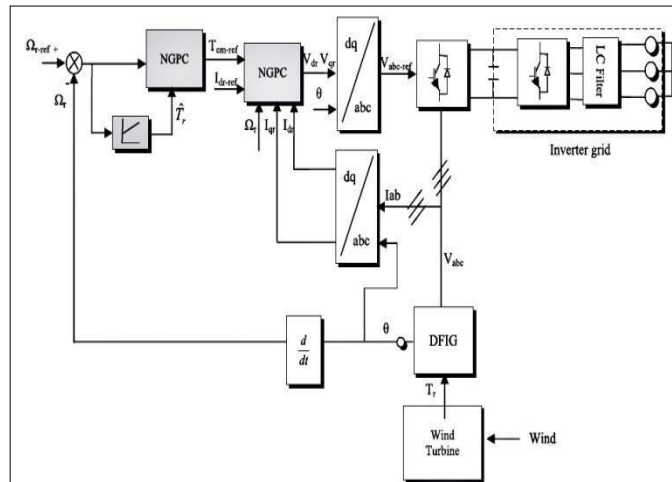


Fig. 4. Cascaded NGPC

**A. Internal control circle**

The plan of this Internal Control circle is to normalize the d-hub rotor current and the electromagnetic force by following upon the rotor armature voltage. The minimal type of Equations (19) and (20) can be composed as follows:

$$\dot{x}(t) = f(x) + gu(x)u(x); y = h(x) \quad (18)$$

With  
:

$$x = \begin{bmatrix} I_{dr} & I_{qr} \\ V_{dr} & V_{qr} \end{bmatrix}; u = \begin{bmatrix} V_{dr} \\ V_{qr} \end{bmatrix}; y = \begin{bmatrix} I_{dr} \\ I_{qr} \end{bmatrix}^T$$

The state vector x is made out of the d-hub and q-pivot segment of the armature rotor flows. The information vector u is ready of the d-pivot and q-hub instrument of the armature rotor voltage. The yield vector y comprises of the electromagnetic force and the d-hub rotor current, while vector work f(x) and g\_u (x) are characterized as:

$$f(x) = \begin{bmatrix} -\frac{R_r}{\sigma L_r} I_{dr} + \omega_s I_{qr} \\ -\frac{R_r}{\sigma L_r} I_{qr} - \omega_s I_{dr} \end{bmatrix}; g_u(x) = \begin{bmatrix} \frac{1}{\sigma L_r} \\ 0 \end{bmatrix} \quad (19)$$

The creations to be prohibited in the internal circle are characterized here:

$$y = h(x) = \begin{bmatrix} I_{dr} \\ I_{qr} \end{bmatrix} = \begin{bmatrix} \frac{1}{\sigma L_r} \\ 0 \end{bmatrix} u$$

$$y_2 = h_2(x) = I_{dr} \quad (20)$$

For the productions  $y_1$  and  $y_2$ , their relative degrees  $\rho_1$  and  $\rho_2$  are equal to 1, as the first derivative reveals the input. The ensuing NGPC functional to the scheme equations gives the control law:

$$u(t) = -G(x)^{-1} \sum_{i=0}^1 \bar{K}_i [L^i h(x) - y^{[i]}(t)] \quad (21)$$

With

$$\bar{K} = \begin{pmatrix} \frac{3}{2T} & 0 \\ 0 & 1 \end{pmatrix} \quad \bar{K} = \begin{pmatrix} 1 & 0 \\ 0 & 1 \end{pmatrix} \quad y = \begin{pmatrix} \omega_r \\ I_{dr} \end{pmatrix} = \begin{pmatrix} \omega_{em-ref} \\ I_{dr-ref} \end{pmatrix}$$

$G(x) = \begin{pmatrix} \omega_s L_s & 0 \\ \sigma L_r & 1 \end{pmatrix}$  and  $T = \begin{pmatrix} T_{em} \\ T_r \end{pmatrix}$  denotes the  $i^{th}$  derivative of  $y(t)$  is the prediction period of the inner loop.

**B. External control circle**

The rapidity regulator in the External circle is secured by allowing for the mechanical dynamics of the TFVIA.

$$J \frac{d}{dt} \Omega_r = T_{em} - T_r - f_r \quad (22)$$

Whereas it follows the nonlinear system form given in equation ( ).

In the generalized form, state vector  $x$  and control input  $u$  are, in that order the rotor speed  $\Omega_r$  also the electromagnetic torque  $T_{em}$ . The output  $y$  is the rotor velocity  $\Omega_r$ ,  $T_r$  is the aerodynamic torque. The vector capacities  $f(x)$ ,  $g_u(x)$  and  $g_T(x)$  are given:

$$f(x) = -\frac{f_r}{J} \quad g_u(x) = \frac{1}{J} \quad g_T(x) = -\frac{1}{J}$$

The relative degree  $\rho$  of the output  $y$  is equal to 1. Then, we shall have the optimal control input as

$$u(t) = -G(x)^{-1} \left[ \sum_{i=0}^1 k_i (L^i h(x) - y^{[i]}(t)) + G(x) T_r(t) \right] \quad (23)$$

with:

$$K_0 = \frac{3}{2T}; \quad K_1 = 1; \quad h(x) = \Omega_r; \quad y_r = \Omega_{r-ref}$$

$$G_u(x) = \frac{\partial h(x)}{\partial x} \quad g_u(x) = \frac{1}{J} \quad G_T(x) = \frac{\partial h(x)}{\partial x} \quad g_T(x) = -\frac{1}{J}$$



ey is the speed tracking error.

## VI. SIMULATION AND RESULTS

Simulation results of the wind turbine for appropriate wind profile, torque profile, tracking performance of the nonlinear observer are obtained. Storm Turbine and TFVIA specifications are shown in table I and table II.

TABLE I. STORM TURBINE PARAMETER

Parameters	Parameter Values
Turbine diameter	60 m
No of blades	3
Hub height	85 m
R	36.5 m
Gear box	90

TABLE II. TWO FOLD VIRTUAL INDUCTION ALTERNATOR PARAMETERS

Parameter	Value	Units
Apparent Power	1500	KVA
Rated Voltage	690	V
Stator resistance ( $R_S$ )	0.0043	pu
Stator reactance ( $L_S$ )	0.0809	pu
Rotor resistance referred to stator side ( $R_r$ )	0.0048	pu
Rotor reactance referred to stator side ( $L_r$ )	0.0871	pu
Magnetizing reactance ( $L_m$ )	3.459	Pu
Frequency (f)	50	Hz
Moment of inertia (J)	0.729	Kg/cm <sup>2</sup>
Pole pairs (P)	3	-
$f_r$	0.0071	-
Relative degree ( $\rho$ )	1	-
Optimal Predictive time for the internal control circle ( $T_{p1}$ )	0.5	ms
Optimal Predictive time for the external control circle ( $T_{p2}$ )	10	Ms

### A. Wind Profile

The Nonlinear predictive controller was designed to withstand in high dynamic variations in the wind profile. So that, the wind profile was chosen with the variations of 16% on wind base speed because wind speed is not allowed by the controller, between the limits 6m/s and 30m/s. Here the wind base speed was chosen as 12m/s. So that, the variations are in between 14 m / s and 10 m / s exposed in fig. 5.

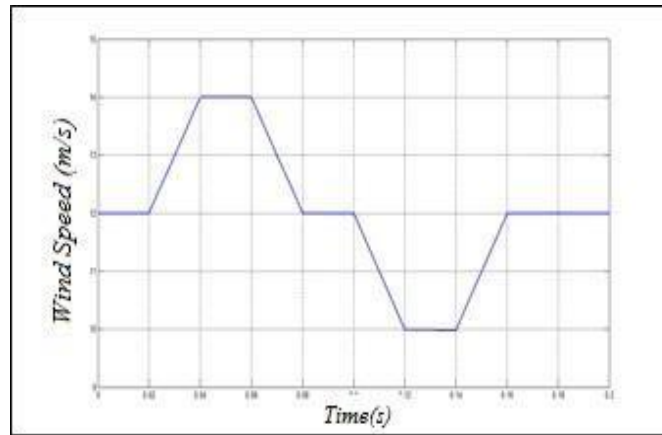


Fig. 5. wind profile

**B. Servo Performance under Unknown Aerodynamic Torque**

The aerodynamic torque variation is tested by checking the tracking performance with the actual aerodynamic torque shown in fig. 6.

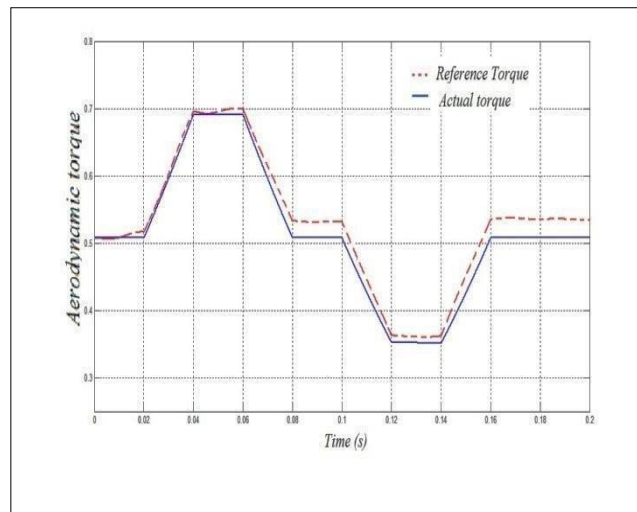


Fig. 6. Actual and estimated aerodynamic torque

To ensure the stability, Lyapunov functions are used. From the Lyapunov stability criterion, the observer gain should be chosen as a negative element is concluded. For various values of the observer gain are tested, the results show that  $\hat{x}(t)$  unites rapidly to

$T_{rt}$  for high estimations of the eyewitness pick up,  $\varphi_0$ . An enormous addition  $\varphi_0$  brings about a quick aggravation dismissal to the disadvantage of the control exertion  $T_{em}$  that is restricted by the velocity channel. At last, the strength of the streamlined force eyewitness is ensured by picking the spectator pick up estimation of  $\varphi_0$  is equivalent to - 3

**C. Tracking Performance of NGPC Outer Loop**

The tracking performance of electromagnetic torque is regulated for various predictive times. However, the tracking performances are satisfied based on the predictive time of the controller. The reference electromagnetic optimally tracks the actual electromagnetic torque for the predictive time of 10ms exposed in fig. 7.

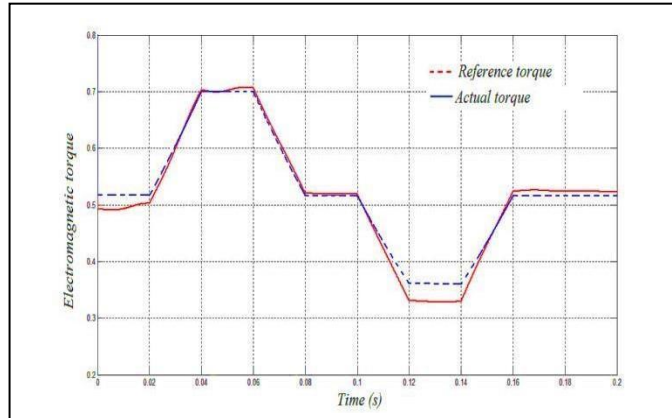


Fig. 7. Actual and Reference electromagnetic Torque

A more modest prescient time brings about a quick aggravation dismissal for the inconvenience for the control  $T_{em}$  which is restricted by the velocity channel.

The Rotor speed error tracking performance is fulfilled for the predictive time 10ms is exposed in fig.8. Based on the error tracking performance of the Rotor generator speed, the aerodynamic torque is estimated in an observer.

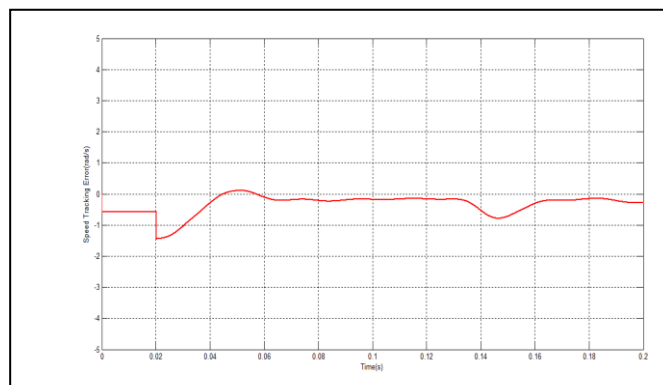


Fig. 8. Speed Tracking Error

**D. NGPC Current Torque Current Control Loop Performance**

The rotor voltages obtained from the controller are shown in fig. 9. The rotor voltage which is given to the converter ensures the maximum voltages, where the voltage fluctuations lead to power fluctuations in the grid. The Predictive time horizon for the controller was concluded as 0.5 ms from the various testing performance of various using different predictive time. At 0.5 ms the voltages obtained as optimal with minimum fluctuations.

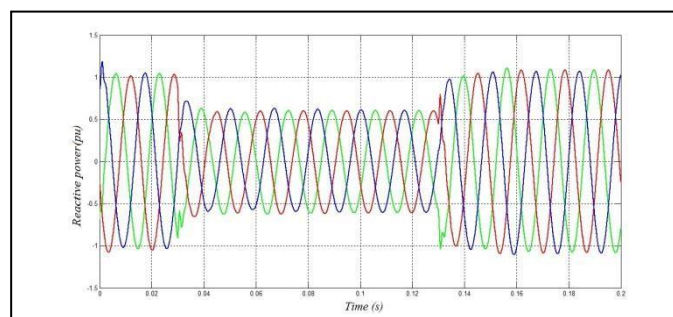


Fig. 9. Reference Rotor Voltage

The matrix net responsive force is kept up at zero worth adding to remunerate the network power factor appeared in fig. 10

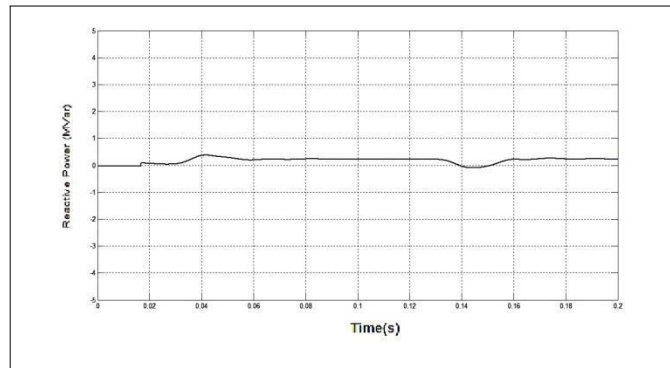


Fig. 10. Grid reactive power

The grid power obtained on the load side is compared with and without Nonlinear predictive Controller is shown in fig.11.

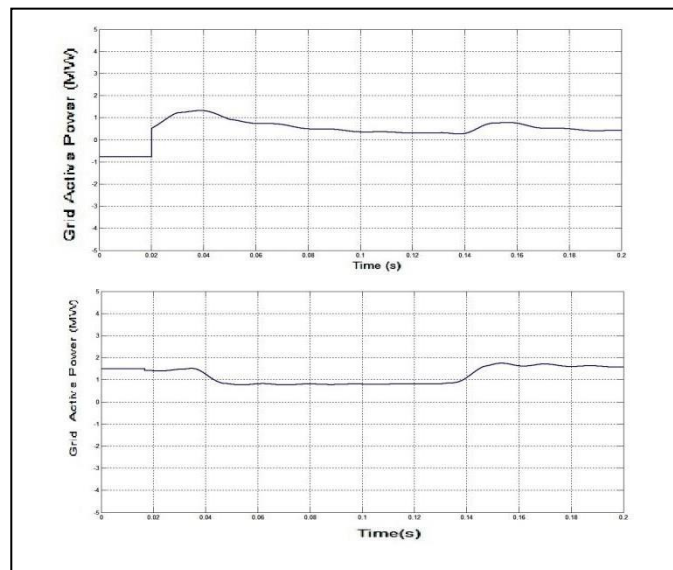


Fig. 11. Grid Active Power without controller and with Controller

## VII. CONCLUSION

A full Nonlinear Generalized Predictive Controller for a Two Fold Virtual Induction Alternator is planned. The control law is induced by advancement of a goal work. It contemplates the control effort and the differentiation between the anticipated yields and the limits like rotor voltage and electromagnetic power, as reference inputs. To ensure the vigor against streamlined force and boundary varieties, an unsettling influence onlooker is planned and incorporated into the control law. Besides, to restrict the control exertion, the reference velocity signal is pursued for the various assessments of gain and prescient time. The recreated yield shows that the matrix dynamic force tracks and it boost the transformation proficiency. From the outcomes, it has been seen that the NGPC with a streamlined force eyewitness gives the better effectiveness and the dependability of the breeze energy conversion frameworks.

## REFERENCES

- [1] olimpo Anaya-lara, nick Jenkins janakaekanayke, phill Cartwright and mike Hughes, *Wind energy generation: Modeling and Control*, Johnwiley publications, 2009
- [2] KamelOuari, ToufikRekioua, and MohandOuhrouche, "Real time simulation of nonlinear generalized predictive control for wind energy conversion system with nonlinear observer," *ISA Trans.*, vol. 53, pp. 76–84, 2014.
- [3] A Tapia, G Tapia, J X Ostoblaza, and J R Saenz, "Modelling and control of a wind turbine driven doubly fed induction generator," *IEEE Trans. on Energy Convers.*, vol. 18, pp. 194-204, 2003.
- [4] L Mihet-Popa, F Blaabjerg, and I Boldea, "Wind turbine generator modeling and simulation where rotational speed is the controlled variable," *IEEE Trans. on Ind. Appl.*, vol. 40, pp. 3-10, 2004.
- [5] Y Coughlan, P Smith, A Mullane and M O'Malley, "Wind turbine modeling for power system stability

- analysis: A system operator perspective,” *IEEE Trans. on Pwr. Syst.*, vol. 22, pp. 929-936, 2007.
- [6] Y.W. Liao, E. Levi, “Modelling and simulation of a stand-alone induction generator with rotor flux oriented control,” *Electric Pwr. Syst. Research*, vol.46, pp. 141–152, 1998.
- [7] H Jiabing, “Direct active and reactive power regulation of DFIG using Sliding-Mode control approach,” *IEEE Trans Energy Convers.*, vol. 25, pp. 1028–1039, 2011.
- [8] F Poitiers \*, T Bouaouiche, M Machmoum, “Advanced control of a doubly-fed induction generator for wind energy conversion,” *Electric Pwr. Syst. Research*, vol. 79, pp. 1085–1096, 2009.
- [9] F Valenciaga, “Second order sliding power control for a variable speed-constant frequency energy conversion system,” *Energy Conversion and Management* vol. 51, pp. 3000-3008, 2010.
- [10] Lie Xu and Yi Wang, “Dynamic modeling and control of DFIG based wind turbines under unbalanced network conditions,” *IEEE Trans. on Pwr. Syst.*, vol. 22, pp. 314-323, Feb, 2007.
- [11] C Belfedal, S Gherbi, M Sedraoui, S Moreau, G Champenois, T Allaoui, and M ADenai, “Robust control of doubly- fed induction generator for standalone applications,” *Energy Pwr. Syst. Res.*, vol. 80, pp. 230-239, Feb, 2010.
- [12] Wen-Hua Chen, Donald J. Balance, and Peter J. Gawthrop, “Optimal control of nonlinear systems: a predictive control approach,” *Automatica*, vol.39, pp.633-641, April, 2003.
- [13] M Nemeč, D Nedeljkovic, and V Ambrožic, “Predictive torque control of induction machines using immediate flux control,” *IEEE Trans. on Ind. Electron.*, vol. 17, pp. 2009-2017, 2010.
- [14] P Correa, M Pacas, and J Rodriguez, “Predictive torque control for inverter fed induction machines,” *IEEE Trans. Ind. Electron.*, vol. 45, pp. 1073-1079, 2007.
- [15] R Hedjar, R Toumi, P Boucher, and D Dumur, “Two cascaded nonlinear predictive controls of induction motor,” *International J. of Comp. Appl.*, vol. 56, pp. 349-365, 2012.
- [16] S Tomonobu, R Sakamoto, N Urasaki, T Funabashi, H Fujita, and H Sekine, “Output power leveling of wind turbine generator for all operating regions by pitch angle control,” *IEEE Trans. on Energy Convers.*, vol. 21, pp. 467-475, 2006.
- [17] S Mostafa, O P Malik, and D T Westwick, “Multiple model predictive control for wind turbines with Doubly fed induction generators,” *IEEE Trans. on Sustain. Energy*, vol. 2, pp. 215-225, 2011.
- [18] Xu Lie, ZhiDawei and Williams Barry, “Predictive current control of doubly-fed induction generators,” *IEEE Trans. on Ind. Electron.*, vol. 56, pp. 4149-4153, 2009.
- [19] W Feng, O’Reilly J, and Donald J Balance, “MIMO Nonlinear PID predictive controller,” *IEE Proc. Control Theory Appl.*, vol. 149, pp. 203–208, 2002.
- [20] Wen-Hua Chen, Donald J. Balance, and Peter J. Gawthrop, “Nonlinear PID predictive controller,” *IEE Proc. Control Theory Appl.*, vol. 146, pp. 603–611, 1999.